Cement and Concrete Research 38 (2008) 976–982

Contents lists available at ScienceDirect

Cement and Concrete Research

journal homepage: http://ees.elsevier.com/CEMCON/default.asp

Influence of additions of coal fly ash and quartz on hydrothermal solidification of blast furnace slag

Z. Jing [c,*], F. Jin [a], T. Hashida [b], N. Yamasaki [c], Emile H. Ishida [c]

[a] State Key Laboratory of Pollution Control and Resources Reuse, College of Environmental Science and Engineering, Tongji University, 1239 Siping Road, Shanghai 200092, China
[b] Fracture and Reliability Research Institute, Tohoku University, Aoba6-6-20, Aoba-ku Sendai 980-8579, Japan
[c] Graduate School of Environmental Studies, Tohoku University, Aoba6-6-20, Aoba-ku Sendai 980-8579, Japan

ARTICLE INFO

Article history:
Received 1 September 2006
Accepted 8 January 2008

Keywords:
Blast furnace slag
Hydrothermal solidification
Tobermorite
Fly ash
Mechanical property

ABSTRACT

Blast furnace water-cooled slag (BFWS) has been solidified hydrothermally with tobermorite formation. The experimental results showed that the addition of fly ash and quartz was favorable to the formation of tobermorite, and the strength development of solidified body depended on both of the tobermorite formation and filling degree of formed tobermorite in the spaces between BFWS particles. The fly ash added appeared to have a higher reactivity than the quartz used during the initial hydrothermal processing due to the higher solubility of glassy phase in fly ash. The tobermorite formation seemed to be very sensitive to the fly ash content, e.g., the addition of fly ash 10–20 mass% was favorable to tobermorite formation, while the excessive addition of fly ash (>20 mass%) appeared to impede the tobermorite formation. The excessive addition of quartz was also shown to exert a negative effect on the tobermorite formation, which causes strength deduction.

1. Introduction

Blast furnace slag (BFS) is a by-product generated in the process of iron ore reduction in blast furnace. More than 24 million tons BFS is generated yearly in Japan, and around 65% of it has been utilized for the manufacture of Portland slag cement [1]. BFS can be divided into air-cooled and water-cooled BFS according to his cooling method, and the blast furnace water-cooled slag comprises nearly 80% of volume of total BFS generated in Japan, which is being used to generate building materials widely [1]. The needs for the cement in Japan have been reduced year by year recently, and in addition large quantities of recycling materials, e.g. coal fly ash, have been also used in these industries. Therefore, there is an urgent requirement to develop a new and environmental acceptable recycling technology for BFS.

BFS, of higher lime content, has a latent hydraulic activity giving rise to its extensive use as a partial replacement for Portland cement. BFS, therefore, may be solidified into building materials directly using a hydrothermal processing method. The hydrothermal processing method has been applied to the field of building materials manufacture for a long time [2], and recently, it has been also used to solidify wastes into building materials, e.g. municipal incineration ash [3], coal fly ash [4], and crushed building and demolition waste [5]. The hydrothermal technology is considered to be suitable for the solidification of BFS in that it can offer both treatment on massive scale and energy saving due to the lower hydrothermal autoclaving temperature ranged typically from 150 to 200 °C. Ishida [2] described that the energy required for the hydrothermal solidification (at 150 °C) of earth (soil) ceramics is only about 1/6th that of energy needed for fired ceramic tiles.

In our previous work, BFS has been solidified firstly using the hydrothermal processing method, and the result showed that the BFS could be solidified with the formation of tobermorite, and the addition of quartz and coal fly ash (as a silica source) into the BFS was shown to be favorable to the tobermorite formation. The solidified body in our study was tough and durable, and therefore the hydrothermal solidification technology may have such a potential for recycling BFS. For coal fly ash, the main components are aluminosilicate glass, mullite and quartz with smaller amounts of residual coal and ore minerals. Because the glassy phase of aluminosilicate usually accounts for 60–80 mass% of fly ash [6], the fly ash may be used as an alternative silica source for the solidification of BFS. The fly ash used for the solidification of BFS, undoubtedly, will offer both resource saving and cost reductions. To the best of our knowledge, however, the hydrothermal solidification of BFS with the addition of fly ash, and the influence of the fly ash added on the hydrothermal solidification of BFS have not been reported extensively in literature.

The present paper is part of an extensive investigation of the hydrothermal solidification of BFS. The objective of the study is to investigate the influence of the fly ash addition on hydrothermal solidification of BFS with comparing with that of the quartz addition. The results are expected to offer useful information on recycling BFS.

2. Experimental

Blast furnace water-cooled slag (BFWS) used in this study was supplied from Sumitomo Metals Ltd. in Japan. The BFWS was ground

* Corresponding author. Tel./fax: +86 21 6598 5792.
E-mail address: zzjing@hotmail.com (Z. Jing).

0008-8846/$ – see front matter © 2008 Elsevier Ltd. All rights reserved.
doi:10.1016/j.cemconres.2008.01.017

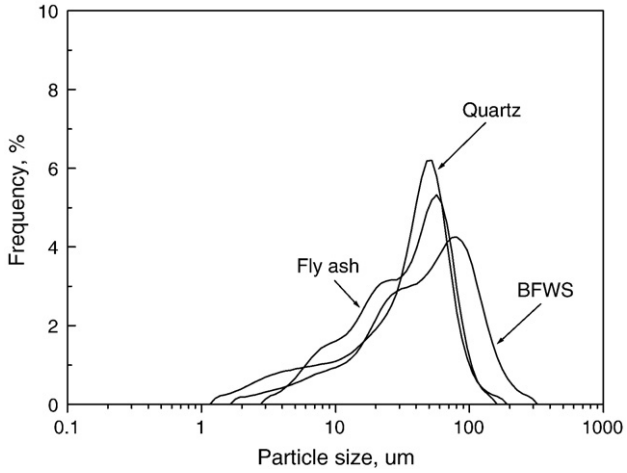

Fig. 1. Particle size distributions of the fly ash, quartz and BFWS used.

with a ball mill. Quartz and fly ash, obtained respectively from the northeast of Japan and a coal-fired power station in Tokyo, were used as additives for the hydrothermal solidification of the BFWS. The particle size distributions of the fly ash, ground quartz and BFWS as determined by laser diffraction technology (X100, Microtrac), and their particle size parameters and BET specific surface areas (ChemBET 3000, Quantachrome) are shown in Fig. 1 and Table 1, respectively. Chemical compositions of the BFWS, quartz and fly ash as determined by X-ray fluorescence (XRF; RIX3100, Rigaku) are shown in Table 2. In order to compare the effect of the fly ash and quartz addition on the hydrothermal solidification of BFWS, the coal fly ash 20 mass% and ground quartz 14 mass% were respectively added into BFWS to make the both starting materials have the same CaO/SiO_2 molar ratio of one. The starting material (20 g) was first mixed manually in a mortar with 5 mass% distilled water (1 ml), and then the mixture was compacted into a disc-shaped mould (30 mm diameter×120 mm height) by compaction pressure of 30 MPa. The demoulded specimens were subsequently autoclaved under the saturated steam pressure (1.56 MPa) at 200 °C, up to 12 h. After autoclaving, all the solidified specimens were dried at 80 °C for 24 h before testing.

The solidified disc-shaped specimens (30 mm diameter×20 mm height) were used to measure the tensile strength employing the Brazilian testing method, which has been adopted as a standard testing method by the International Society for Rock Mechanics [7]. The Brazilian tests were conducted in an Instron universal testing machine (M1185) at a crosshead speed of 0.2 mm/min. Each experimental result quoted in this study was the average of three specimens from the same hydrothermal processing condition. After the Brazilian testing, the crushed specimens were investigated using several techniques. The phase analysis was determined by an X-ray diffraction (XRD, MiniFlex, Rigaku), using Ni-filtered Cu K_α radiation and operating with voltage of 30 kV and emission current of 15 mA. The step scan covered the angular range of 5–65° (2θ) at a scan rate of 2° (2θ) per minute. The microstructure was observed by a scanning electron microscope (SEM, S-4100, Hitachi), which was conducted at an accelerating voltage of 5 kV. The porosity and pore size distribution

Table 1
Particle size parameters and specific surface areas of the fly ash, quartz and BMWS used

	$D(10)$[a], μm	Median size $D(50)$, μm	$D(90)$[b], μm	BET surface area, m^2/kg
Fly ash	8.5	33.8	72.1	2100
Quartz	5.3	36.6	69.9	2700
BFWS	9.7	46.3	115.5	370

[a] $D(10)$ means 10% of the powder particles are smaller than this value.
[b] $D(90)$ means 90% of the powder particles are smaller than this value.

Table 2
Compositions of the BFWS, quartz and fly ash used (mass%)

	BFWS	Quartz	Fly ash
SiO_2	32.6	89.7	53.1
CaO	44.7	0.91	3.5
Al_2O_3	15.8	7.02	24.0
MgO	3.5		0.61
SO_3	1.2		0.08
Mn_2O_3	0.3		
TiO_2	1.1	0.25	4.58
Fe_2O_3		0.62	5.1
Ig-loss	0.8	1.5	9.03

were measured by a mercury intrusion porosimetry (MIP, Poremaster-33, Quantachrome), which had a measuring pressure ranging from 0.86–200 MPa. The contact angle and surface tension selected were respectively taken as 140° and 0.48 N/m, and the measurable pore size ranged from 6.4 nm to 175 μm. The samples (~0.23 cm^3) were dried in an oven at 80 °C for 48 h before testing, and only intrusion (continuous method) testing was carried out in this study.

3. Results and discussion

3.1. Mechanical property

Fig. 2 indicates the XRD patterns of the BFWS and fly ash used. The absence of any sharp diffraction peaks with a typical background

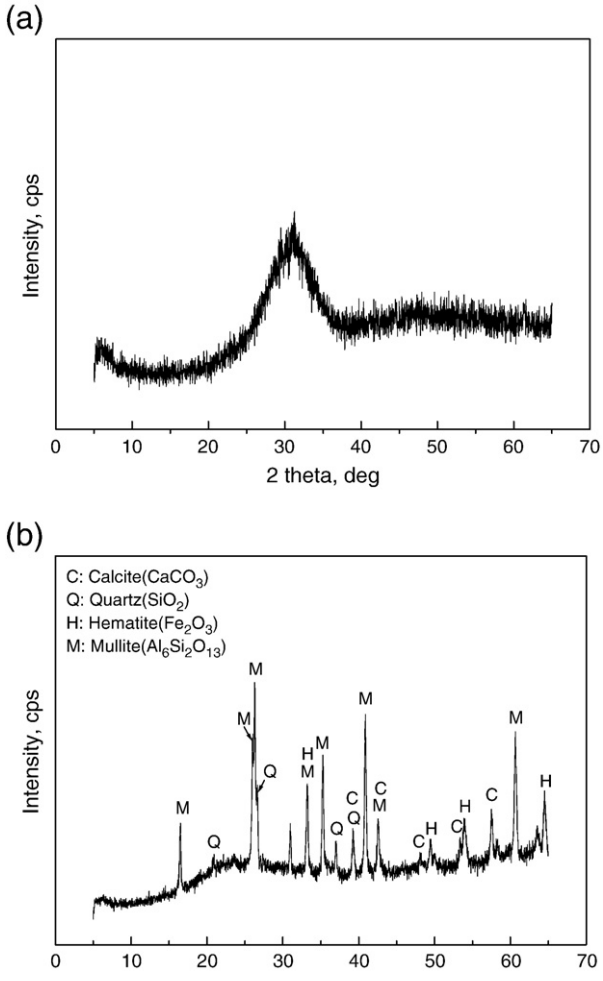

Fig. 2. XRD patterns of the fly ash and BFWS. (a) BFWS; (b) fly ash.

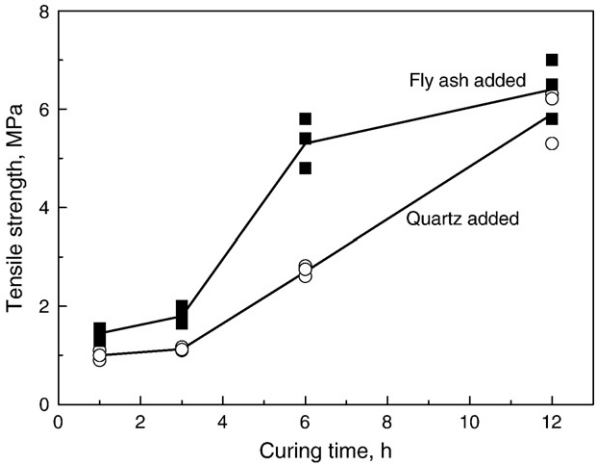

Fig. 3. Influence of curing time on the strength development of the solidified specimens synthesized at 200 °C, with fly ash 20 mass% and quartz 14 mass%. Square (■) and circle (○) marks are the measured values for fly ash and quartz added at each condition respectively, and the lines between the marks are the average tensile strengths based on these three measured samples.

feature denotes that the BFWS is almost entirely amorphous. For the XRD pattern of the fly ash, main phases corresponding to mullite ($3Al_2O_3{\cdot}2SiO_2$), quartz (SiO_2), hematite (Fe_2O_3) and calcite ($CaCO_3$) are confirmed, and the broad hump of XRD base line indicates the presence of amorphous phase in the original fly ash.

The strength development with curing time is shown in Fig. 3. In both cases of the fly ash (20 mass%) or quartz (14 mass%) added, the tensile strengths increase with increasing curing time, in which the increase in strength is initially slow in the first 3 h, and becomes quick afterwards. The tensile strengths at 12 h are approximately 6 MPa (~12 MPa in flexural strength) for the two cases of the fly ash and quartz added. It should be noted that there exists a significant difference in the strength development, e.g., the largest difference in the strength occurs at 6 h, while the difference tends to decrease until 12 h. Because the powder properties of the fly ash and quartz added are similar (BET surface area of the quartz used is even higher then that of the fly ash), this suggests that the fly ash added appears to be more reactive than quartz, which has promoted the strength development in a shorter time.

3.2. XRD analysis

The phase changes during the evolution of the strength with curing time and temperature were determined by XRD (Fig. 4). The XRD pattern for curing time of 0 h corresponds to the specimen before hydrothermal processing. Mullite, quartz and calcite as the main phases for initial specimen synthesized with fly ash are

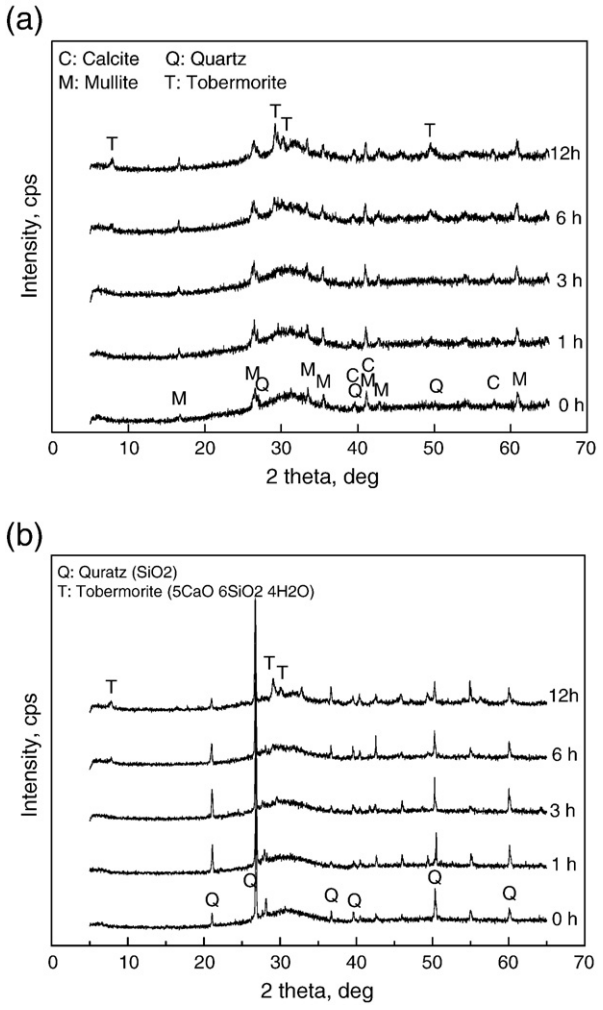

Fig. 4. Evolutions of the XRD patterns with curing time for the solidified specimens synthesized with fly ash 20 mass% and quartz 14 mass%. (a) fly ash added; (b) quartz added.

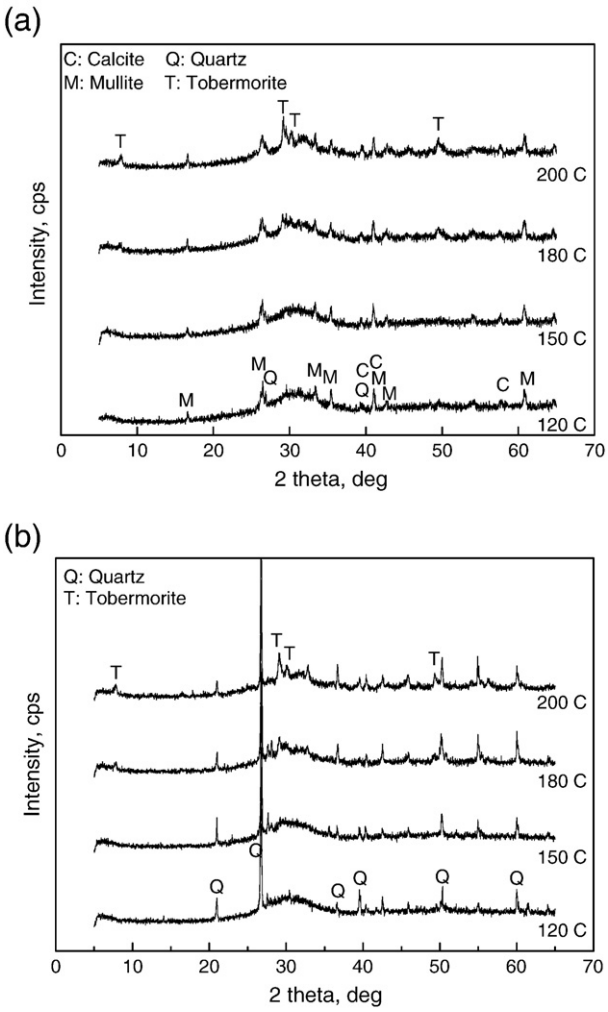

Fig. 5. Evolutions of the XRD patterns with curing temperature for the solidified specimens synthesized with fly ash 20 mass% and quartz 14 mass%. (a) fly ash added; (b) quartz added.

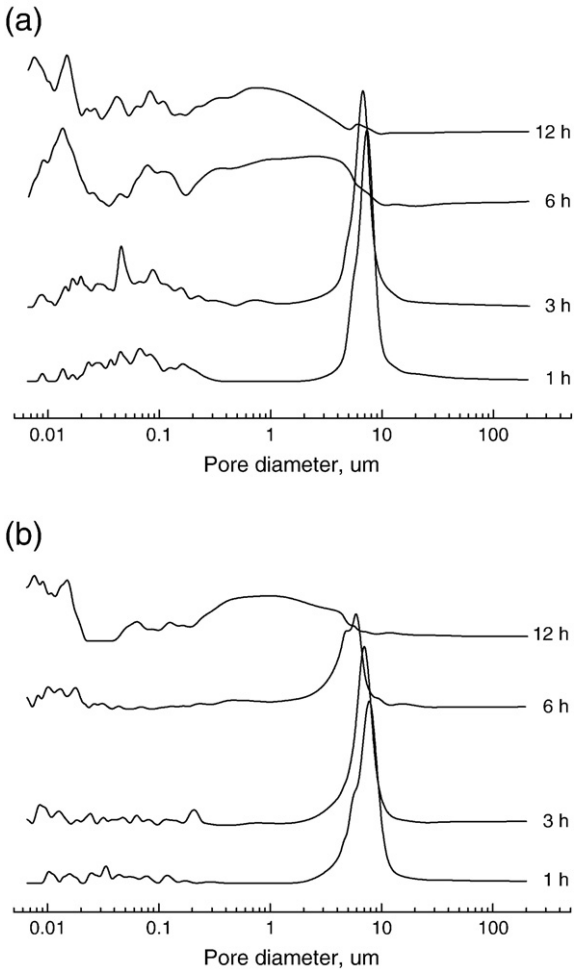

Fig. 6. Evolutions of pore size distributions of the solidified specimens with curing times by addition of the fly ash 20 mass% and quartz 14 mass%. (a) fly ash added; (b) quartz added.

confirmed (Fig. 4(a)). The evolution of XRD patterns with increasing curing time shows that the peak intensities of mullite keep almost unchanged, indicating that the mullite is stable during hydrothermal processing. Catalfamo et al. [8] and Berkgaut and Singer [9] also reported the stability of mullite during hydrothermal treatment. It is notable that a new phase corresponding to 1.1 nm tobermorite ($Ca_5(OH)_2Si_6O_{16}{\cdot}4H_2O$) forms from 6 h concurrently. Compared with the strength development shown in Fig. 3, the tobermorite formation is believed to enhance the strength. Tobermorite is a calcium silicate hydrate mineral of ideal composition $Ca_5(OH)_2Si_6O_{16}{\cdot}4H_2O$ and it can be formed by hydrothermal reaction between dissolved silica and calcium. Owing to the high content of aluminosilicate glass in the fly ash and the stability of mullite during hydrothermal processing, the silica for the tobermorite formation appears to come mainly from the amorphous silica in the fly ash. Inada et al. [10] also reported that the glassy phase of fly ash could be used for formation of zeolite in hydrothermal process. In contrast, for the case of quartz added, the peak intensities of quartz (Fig. 4(b)) seem to be almost unchanged only during the first 3 h and decrease from 6 h, and at the same time a phase of 1.1 nm tobermorite becomes distinct. The decrease in the peak intensity of quartz is due clearly to the fact that some of the quartz has been reacted to form 1.1 nm tobermorite. According to the strength evolution shown in Fig. 3, the fly ash seems to be more reactive than quartz, which has supplied more silica available to react with calcium to form more tobermorite at a shorter curing time, however, with increasing time more calcium consumption inevitably lowers the pH of pore solution, thus affecting the further hydrothermal reaction speed. For the addition of fly ash and quartz, the longer curing time (12 h) appears to lead to more tobermorite formation, thus further enhancing the strength (Fig. 3).

The evolution of the XRD patterns with curing temperature is shown in Fig. 5. At 120 °C, the main phases of mullite, quartz, calcite, and quartz are confirmed for the specimens synthesized with the fly ash and quartz, respectively. However, at 180 °C, a trace of phase of 1.1 nm tobermorite is confirmed for the both cases of the fly ash and quartz added, and their peak intensities increase with curing temperature increasing.

3.3. Microstructural evolution

Detailed investigation of the microstructure evolution with curing time was conducted by measuring the pore diameter distribution within the specimens (Fig. 6). At curing time of 1 h, the pore size distribution gives the highest frequency distribution peak at 7 μm for the specimen synthesized with the fly ash (Fig. 6(a)). The peaks keep almost same until curing time of 3 h, however, they change thoroughly afterwards, and at the same time new peaks at ~0.01 μm form. The peak of pore distribution corresponds to the space dimensions between the particles within specimen at the time of their formation. The peak shift and formation suggest that the formed crystals have filled in the spaces between particles. According to the XRD results shown in Fig. 4 (a), the new-formed crystals consist mainly of 1.1 nm tobermorite. As shown in Fig. 6, the pores mainly distribute into two parts, i.e. micropore (<0.1 μm) and macropore (>0.1 μm) distribution.

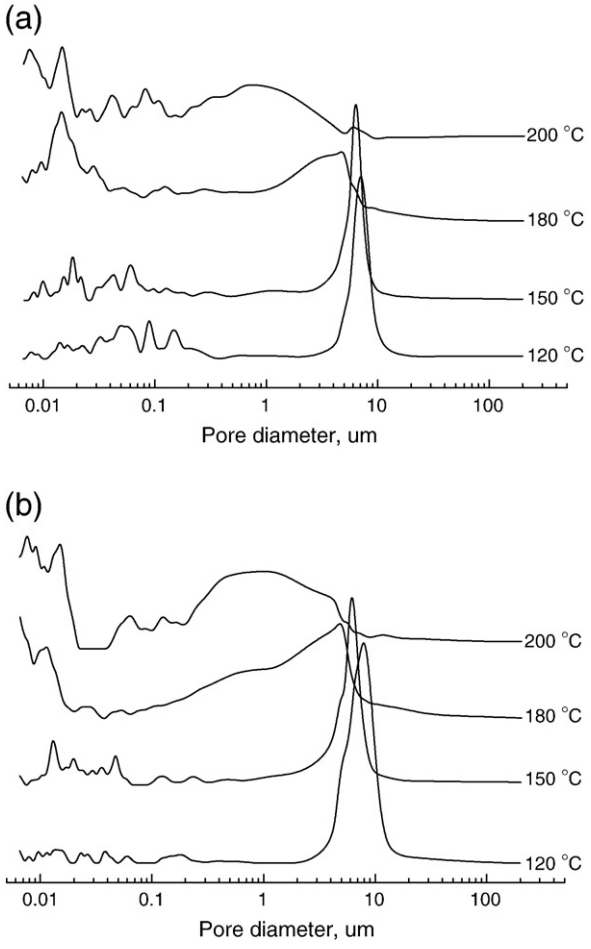

Fig. 7. Evolutions of pore size distributions of the solidified specimens with curing temperature by addition of the fly ash 20 mass% and quartz 14 mass%. (a) fly ash added; (b) quartz added.

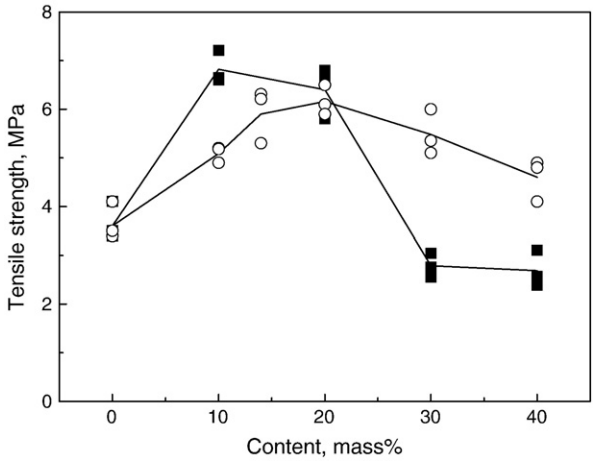

Fig. 8. Effects of the addition contents of the fly ash and quartz on the tensile strength of solidified specimens. Square (■) and circle (○) marks are the measured values for the fly ash and quartz added at each condition respectively, and the lines between the marks are the average tensile strengths based on these three measured samples.

The peaks shifted and widened in the range of macropore suggest that lots of crystals have filled in the spaces between particles, while the peaks formed in the range of micropore reflect the new-formed intercrystalline spaces. The peak at ~0.01 μm may correspond to the formation of tobermorite (the micro space of intercrystalline tobermorite), in agreement with the results reported by Mitsuda et al. [11] and Maenami et al. [12]. Fig. 6(b) shows the evolution of the pore size distribution with curing time for the specimens synthesized with the quartz. A significant difference from Fig. 6(a) is that only a small peak shift occurs at 6 h for the quartz added (at 12 h the peak changes greatly), indicating that the formed tobermorite is insufficient for the peak shift and formation. A trace of tobermorite is confirmed by XRD analysis for the both cases of the fly ash and quartz added at curing time of 6 h (Fig. 4), and the microstructure investigation (pore size distribution), however, appears to provide more information on the filling degree of the formation of crystals (tobermorite). The addition of fly ash, clearly, provides much more tobermorites than the addition of quartz, which fills in the space between particles, and in turn results in a higher strength at 6 h shown in Fig. 3.

The evolutions of the pore distribution with curing temperature were also carried out for the additions of the fly ash and quartz (Fig. 7). In both cases of the fly ash and quartz added, the trends of pore distribution changes with curing temperature are similar, e.g., from 180 °C, the formed crystals lead to a shift of macropore distribution peak towards to a smaller pore diameter, and a formation of micropore distribution peak.

3.4. Addition contents of fly ash and quartz

In order to further investigate the influence on the solidification of BFWS for the two cases of the fly ash and quartz used, the effect of the addition content of the fly ash and quartz on the strength of the hydrothermal solidified specimen was conducted (Fig. 8). The experiments were carried out under the same conditions as before, except the addition contents of fly ash and quartz. The strengths increase first, and then decrease, which indicates an optimum content for the solidification of BFWS. The maximum strength achieved for the addition content of the fly ash is 10 mass%, while that for the quartz is 20 mass%, suggesting a higher reactivity for the fly ash used. The optimum strength is between 10–20 mass% for both quartz and fly ash additions in this study, which appears to be similar to the observation [13] that the highest strength for the autoclaved blended cement (cement+finely ground silica) was obtained at a quartz/cement weight ratio of about 30/70. It is notable that the strength decreases quickly after the fly ash of 20 mass% added.

The effect of the fly ash and quartz content on the strength development was also determined by XRD analysis (Fig. 9). Without addition of fly ash (Fig. 9(a)), the main phase corresponding to hibschite ($Ca_3Al_2(SiO_4)_{3-x}(OH)_{4x(x=0.2-1.5)}$) is distinct. After addition of fly ash, besides some phases of mullite, quartz and calcite, a new phase of 1.1 nm tobermorite becomes discernible, and from 30 mass%, however, the peak of tobermorite becomes much less distinct. Comparison between the XRD results and the strength results shown in Fig. 8 reveals that the strength reduction at fly ash 30 mass% is due to no tobermorite formed within the solidified specimen to support the strength. With addition of quartz (Fig. 9(b)), besides quartz phases, tobermorite phases are observed for quartz content from 10 to 40 mass%.

Fig. 10 shows the pore size distributions of the solidified specimens synthesized with different fly ash and quartz contents. With the fly ash addition 0 mass%, the pore distribution peak is of 7 μm, which changes thoroughly for the addition of fly ash from 10 to 20 mass% (Fig. 10(a)), suggesting that a lot of crystals (tobermorite) have formed (new-formed peaks in the micropore distribution) and the formed crystals have filled in the space between particles (main peak shifts to the smaller pore size). However, the pore size distributions for the fly ash addition between 30 and 40 mass% become similar to that without the fly ash added, and their peaks only have a small shift to the finer pore size. Clearly, the excessive addition of fly ash is unfavorable to the tobermorite formation, and the small shift is due possibly to more fly ash introduction whose particle size is finer than BFWS's (Table 1). With the addition of quartz (Fig. 10(b)), the pore size distributions

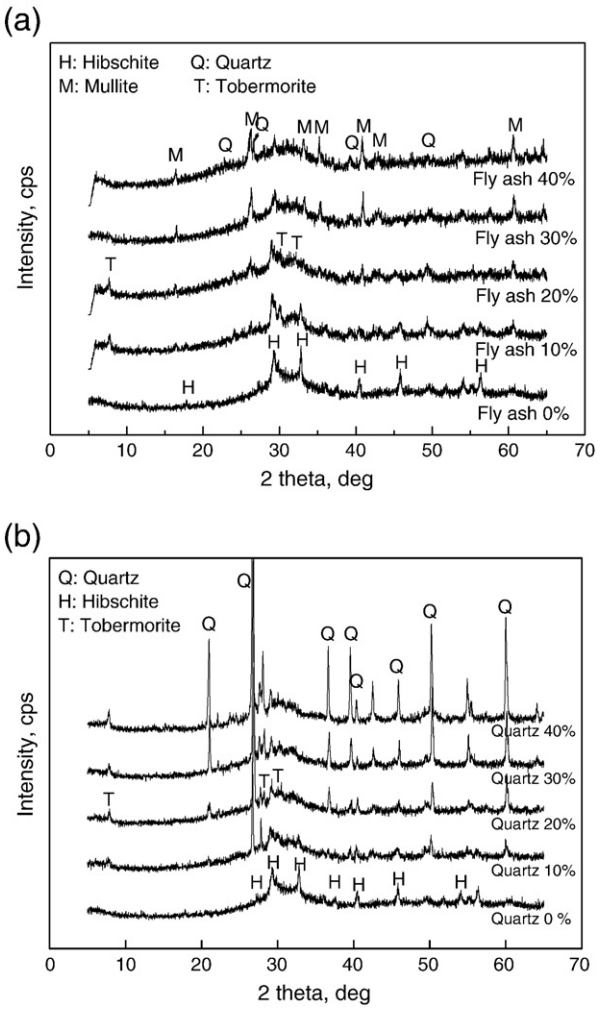

Fig. 9. Evolution of the XRD patterns with content. (a) fly ash added; (b) quartz added.

change greatly. It should be noted that both of the macropore and micropore size distributions with the quartz contents of 20–40 mass% tend to shift toward the larger pore size. This suggests that the new-formed intercrystalline spaces become larger (filling degree of tobermorite formed becomes smaller) and the amount of tobermorite filled in the spaces between particles becomes fewer with increasing quartz content, which reveals that the strength enhancement depends mainly on both of tobermorite formation and filling degree of tobermorite formed in the spaces between BFWS particles. This also indicates that the excessive addition quartz affects the formation of tobermorite, and in turn exerts a minus influence on the strength development.

Fig. 11 shows SEM photographs of the fracture surface of solidified specimens for the fly ash addition of 20 and 40 mass%. An overgrowth of fibrous tobermorite forms for the addition of the fly ash 20 mass% (Fig. 11(a)), which bonds particles together and fills in the spaces between particles; while only few fibrous crystals can be observed for the addition of the fly ash 40 mass% (Fig. 11(b)), and a lot of fly ash particles are also observed in the specimen. These SEM photographs clearly reveal the difference in the pore size distribution for the fly ash addition of 20 and 40 mass% shown in Fig. 10(a), which results in the different strength development shown in Fig. 8.

As shown in Table 1, the particle size parameters of the fly ash and quartz are similar, and the BET specific surface area of the fly ash is even smaller than that of the ground quartz. In addition, the Ca/Si molar ratio of the starting materials for the addition of quartz 14 mass% and flay ash

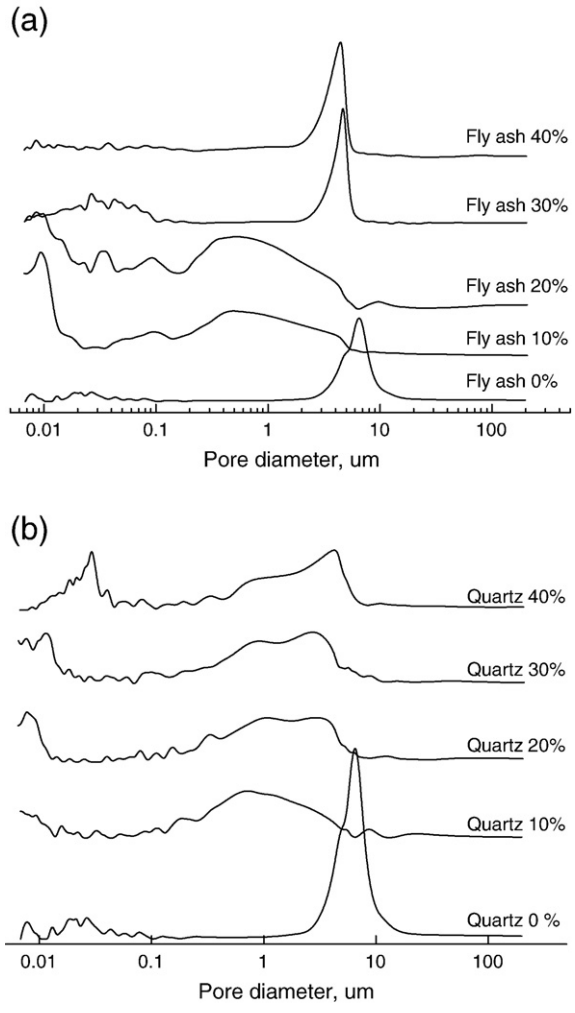

Fig. 10. Evolutions of pore size distributions of the solidified specimens with content. (a) fly ash added; (b) quartz added.

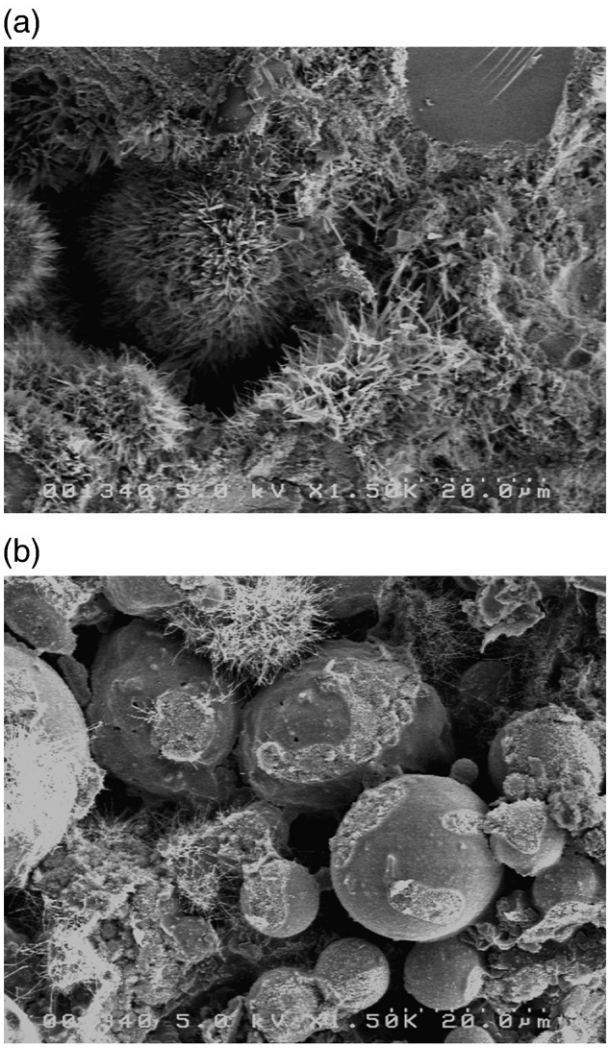

Fig. 11. SEM photographs of the solidified specimens synthesized with the fly ash added. (a). 20 mass%; (b). 40 mass%.

20 mass% is the same (Ca/Si = 1). As discussed above, the fly ash added seems to have a higher hydrothermal reactivity than the quartz, which is capable of supplying more silica available to form tobermorite at a shorter time. However, the tobermorite formation appears to be very sensitive to the fly ash content. Addition content of the fly ash 10–20 mass% was proved to be favorable to the tobermorite formation, while the excessive addition (>20 mass%) of the fly ash seemed to impede the tobermorite formation. The excessive addition of the quartz also affects the tobermorite formation, which also exerts a minus influence on the hydrothermal solidification of BFWS.

4. Conclusions

BFWS has been solidified with a hydrothermal processing method by the additions of fly ash and quartz, and the experimental results can be summarized as follows:

(1) BFWS could be solidified hydrothermally by the additions of the fly ash and quartz. The addition of the fly ash or quartz was shown to be favorable to the tobermorite formation during the hydrothermal process.
(2) The strength development depended on both the formation of tobermorite and filling degree of the formed tobermorite in the space between particles within the solidified specimen.

(3) The fly ash used appeared to have a higher reactivity than the quartz during the initial hydrothermal processing due to the higher solubility of glass phase in fly ash, which seemed to provide more silica available for tobermorite formation.
(4) Tobermorite formation was very sensitive to the addition content of fly ash, e.g., a suitable addition of fly ash (10–20 mass%) was proved to be favorable to the tobermorite formation, while the excessive addition of the fly ash seems to impede the tobermorite formation, thus exerting a significant minus influence on the strength development.
(5) Addition of quartz was favorable to the tobermorite formation; however, the excessive addition of quartz exerted a minus effect on the tobermorite formation, which causes strength decrease.

Acknowledgment

The work reported here was partially supported by the Iron and Steel Institute of Japan under grand of 45310244.

References

[1] Annual Report of Japanese Ceramic Industry 2004, Ceramics Japan 40(9) (2005) 703–744.
[2] Emile H. Ishida, Soil-ceramics (earth), self-adjustment of humidity and temperature, Encyclopedia of Smart Materials, Mel Schwartz, 2002, pp. 1015–1029.
[3] Z. Jing, N. Matsuoka, F. Jin, T. Hashida, N. Yamasaki, Municipal incineration bottom ash treatment using hydrothermal solidification, Waste Manage. 27 (2007) 287–293.
[4] Z. Jing, N. Matsuoka, F. Jin, N. Yamasaki, K. Suzuki, T. Hashida, Solidification of coal fly ash using hydrothermal processing method, J. Mater. Sci. 41 (2006) 1579–1584.
[5] H.M.L. Schuur, Calcium silicate products with crushed building and demolition waste, J. Mater. Civ. Eng. 12 (4) (2000) 282–287.
[6] G.J. McCarthy, J.K. Solem, X-ray diffraction analysis of fly ash. II. Results, Adv. X-ray Anal. 34 (1991) 387–394.
[7] International Society for Rock Mechanics Commission on Standardization of Laboratory and Field Tests, Suggested methods for determining tensile strength of rock materials, Int. J. Rock Mech. Min. Sci. Geomech. Abstr. 15 (1978) 99–103.
[8] P. Catafamo, F. Corigliano, P. Primerano, S.D. Pasquale, Study of the pre-crystallization stage of hydrothermally treated amorphous aluminosilicates through the composition of the aqueous phase, J. Chem. Soc., Faraday Trans. 89 (1993) 171–175.
[9] V. Berkgaut, A. Singer, High capacity cation exchanger by hydrothermal zeolitization of coal fly ash, Appl. Clay Sci. 10 (1996) 369–378.
[10] M. Inada, H. Tsujimoto, Y. Eguchi, N. Enomoto, J. Hojo, Microwave-assisted zeolite synthesis from coal fly ash in hydrothermal process, Fuel 84 (2005) 1482–1486.
[11] T. Mitsuda, K. Sasaki, H. Ishida, Phase evolution during autoclaving process of aerated concrete, J. Am. Ceram. Soc. 75 (7) (1992) 1858–1863.
[12] H. Maenami, O. Watanabe, H. Ishida, T. Mitsuda, Hydrothermal solidification of kaolinite–quartz–lime mixtures, J. Am. Ceram. Soc. 83 (2000) 1739–1744.
[13] H.F.W. Taylor, Cement Chemistry, Academic Press, New York, 1990, pp. 365–367.